Fifth International Conference on
Recent Advances in Geotechnical Earthquake Engineering and Soil Dynamics
and Symposium in Honor of Professor I.M. Idriss
May 24-29, 2010 • San Diego, California

ON THE INFLUENCE OF THE GRAIN SIZE DISTRIBUTION CURVE ON DYNAMIC PROPERTIES OF QUARTZ SAND

Torsten Wichtmann
Institute of Soil Mechanics and Rock Mechanics
University of Karlsruhe, Germany

Theodor Triantafyllidis
Institute of Soil Mechanics and Rock Mechanics
University of Karlsruhe, Germany

ABSTRACT

The paper reports on our effort to extend the well-known Hardin's equation by the influence of the grain size distribution curve. The study is motivated by the fact that Hardin's equation with its commonly used constants can significantly over-estimate the small strain shear modulus G_{max} of well-graded sands. Approximately 350 resonant column (RC) tests with additional P-wave measurements have been performed on 33 specially mixed grain size distribution curves of a quartz sand with different mean grain sizes d_{50}, coefficients of uniformity $C_u = d_{60}/d_{10}$ and fines contents FC. The experiments show that for constant values of void ratio and pressure, the shear modulus G_{max} and the small-strain constrained elastic modulus M_{max} are independent of the mean grain size, but strongly decrease with increasing coefficient of uniformity. A fines content further reduces the small-strain stiffness. In order to improve the estimation of G_{max} and M_{max}, the parameters of Hardin's equation have been correlated with C_u and FC. A correlation of G_{max} and M_{max} with relative density D_r is less accurate. For a certain shear strain amplitude γ, the modulus degradation factor $G(\gamma)/G_{max}$ is smaller for higher C_u-values but does not depend on the fines content. An extension of an empirical formula for the modulus degradation factor is presented.

INTRODUCTION

For feasibility studies, preliminary design calculations or final design calculations in small projects dynamic soil properties are often estimated by means of empirical formulas.

The secant shear modulus G is usually described as a product of its maximum value G_{max} at very small shear strain amplitudes γ and a modulus degradation factor $F(\gamma)$:

$$G = G_{max}\, F(\gamma) \tag{1}$$

Eq. (1) considers that the secant shear modulus decreases with γ if a certain threshold value ($\gamma \approx 0.001$ % for sand) is surpassed.

A widely used empirical formula for the small strain shear modulus G_{max} of sand is one proposed by Hardin and Richart (1963) and Hardin and Black (1966) (given here in its dimensionless form):

$$G_{max} = A\, \frac{(a-e)^2}{1+e}\, (p_{atm})^{1-n}\; p^n \tag{2}$$

with void ratio e, mean pressure p and atmospheric pressure p_{atm} = 100 kPa. The constants A = 690, a = 2.17 and n = 0.5 for round grains, and A = 320, a = 2.97 and n = 0.5 for angular grains were recommended by Hardin and Black (1966) and are often used for estimations of G_{max}-values for various sands.

An alternative formula was proposed by Seed and Idriss (1970) (see also Seed et al. (1986), here converted to SI units):

$$G_{max} = 218.8\; K_{2,max}\; p^{0.5} \tag{3}$$

with G_{max} and p in [kPa] and with a dimensionless modulus coefficient $K_{2,max}$. Seed et al. (1986) stated that $K_{2,max}$-values obtained from laboratory tests range from about 30 for loose sands to about 75 for dense sands.

For the modulus degradation factor $F(\gamma)$ in Eq. (1) Hardin and Drnevich (1972) proposed the following function:

$$F(\gamma) = \frac{1}{\dfrac{\gamma}{\gamma_r}\left[1 + a \exp\left(-b\,\dfrac{\gamma}{\gamma_r}\right)\right]} \tag{4}$$

with a reference shear strain amplitude γ_r and two constants a and b. The reference amplitude γ_r is defined as

$$\gamma_r = \tau^{\max} / G_{\max} \qquad (5)$$

with $\tau^{\max}$ being the shear strength.

Eq. (2) with its commonly used constants does not consider the strong dependence of the small strain shear modulus on the grain size distribution curve. A respective literature review has been given by Wichtmann and Triantafyllidis (2009a). Fig. 1 presents test results of Iwasaki and Tatsuoka (1977). They demonstrated that $G_{\max}$ does not depend on the mean grain size but strongly decreases with increasing coefficient of uniformity $C_u = d_{60}/d_{10}$ and with the fines content FC. Iwasaki and Tatsuoka (1977) performed a single test on each sand. They did not extent Eq. (2) by the influence of C_u and FC. However, their experiments demonstrated that Hardin's equation with its commonly used constants can significantly overestimate the small-strain stiffness of well-graded sands. Therefore, an extension of Eq. (2) by the influence of the grain size distribution curve is necessary. It is the purpose of the present study.

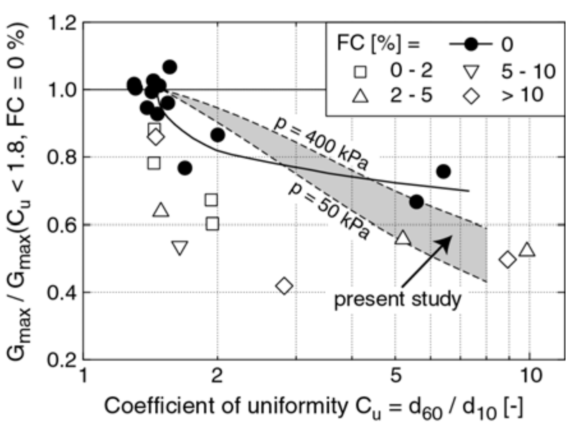

Fig. 1: Decrease of G_{max} with increasing coefficient of uniformity C_u and with increasing fines content FC, test results of Iwasaki and Tatsuoka (1977) compared to results of the present study

TESTED MATERIAL

A natural quartz sand obtained from a sand pit near Dorsten, Germany was sieved into 25 single gradations with grain sizes between 0.063 mm and 16 mm. The grains have a subangular shape and the specific weight is $\rho_s = 2.65$ g/cm^3. From these gradations the grain size distribution curves shown in Fig. 2 were mixed.

28 grain size distribution curves (materials L1 to L28, Fig. 2a-c) were mixed without a content of fines. They are linear in the semi-logarithmic scale. Nine sands or gravels (L1 to L9, Fig. 2a) had different mean grain sizes in the range 0.1 mm $\leq d_{50} \leq$ 6 mm and a coefficient of uniformity of $C_u = 1.5$. The gravel L9 was too coarse to be tested in the RC device (specimen diameter d = 10 cm).

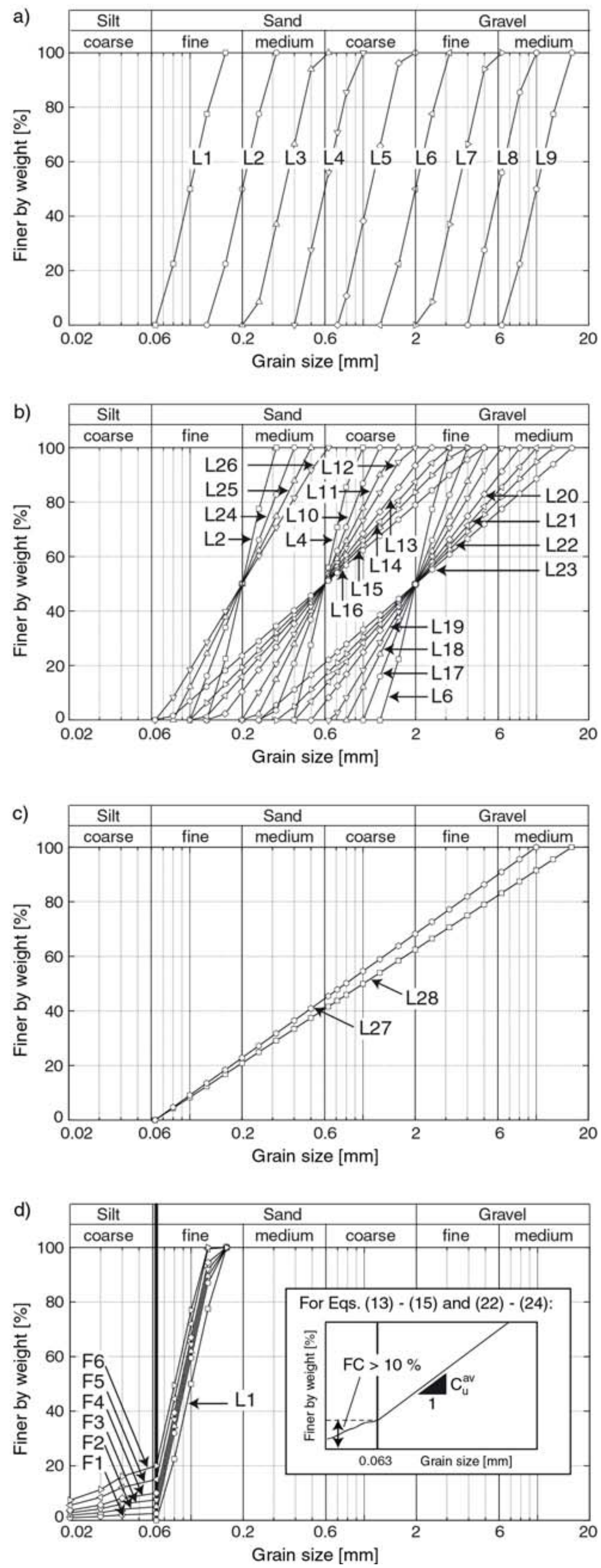

Fig. 2: Tested grain size distribution curves

The mean grain sizes of the sands L10 to L26 (Fig. 2b) were d_{50} = 0.2, 0.6 or 2 mm, respectively, while the coefficients of uniformity varied in the range $2 \leq C_u \leq 8$. Two sand-gravel mixtures (L27 and L28, Fig. 2c) with larger coefficients of uniformity (C_u = 12.6 or 15.9) were also tested.

The influence of the fines content (= percentage of grains with diameters $d < 0.063$ mm) was tested by means of the six grain size distribution curves F1 to F6 shown in Fig. 2d. The fines content was varied in the range $0\ \% \leq FC \leq 20\ \%$. For the fines content a quartz meal was used. In the range $d > 0.063$ mm the grain size distribution curves of the sands F1 to F6 are parallel to those of the materials L1 to L9 (C_u = 1.5).

TEST DEVICE, SPECIMEN PREPARATION AND TESTING PROCEDURE

The resonant column device used for the present study (Fig. 3) belongs to the "free-free" type, that means both, the top and the base mass are freely rotatable. The cylindrical specimens with full cross section measured 10 cm in diameter and 20 cm in height. The system consisting of the specimen and the end masses is encompassed in a pressure chamber. A small anisotropy of stress results from the weight of the top mass (m ≈ 9 kg). The torsional excitation is generated by a pair of electrodynamic exciters integrated into the top mass. The excitation frequency was varied until the resonant frequency was found. The small-strain shear modulus was calculated from the resonant frequency. The test device and the determination of the dynamic soil properties has been explained in detail by Wichtmann and Triantafyllidis (2009a).

The P-wave velocity was measured by means of a pair of piezoelectric elements integrated into the specimen end plates (Fig. 3). The travel time was determined from a comparison of the single sinusoidal signal transmitted at the bottom of the specimen and the signal received at the top plate. The measuring equipment and the analysis of the signals has been presented in detail by Wichtmann and Triantafyllidis (2009b).

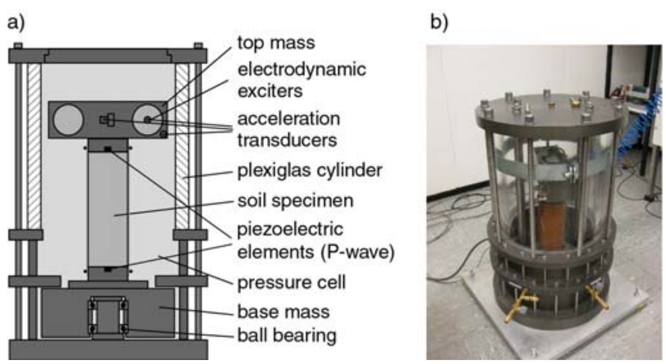

Fig. 3: a) Scheme and b) photo of the resonant column (RC) device used for the present study

The specimens were prepared by dry pluviation of sand out of a funnel into split moulds. For each grain size distribution curve several specimens with different initial relative densities D_{r0} were tested. The isotropic stress was increased in seven steps from p = 50 to p = 400 kPa. At each pressure the small-strain shear modulus $G_{\max}$ and the P-wave velocity v_P were measured. At p = 400 kPa the curves of shear modulus and damping ratio versus shear strain amplitude were determined. In three additional tests the curves $G(\gamma)$ and $D(\gamma)$ were measured also at smaller pressures p = 50, 100 and 200 kPa. Medium dense specimens were used for these tests.

Deformations due to the increase of pressure and the onset of settlement during the increase of the shear strain amplitude were measured by means of non-contact displacement transducers.

TEST RESULTS

Influence of d_{50} and C_u on $G_{\max}$

Exemplary for sand L4, Fig. 4 shows the well-known increase of the small-strain shear modulus $G_{\max}$ with decreasing void ratio e and with increasing mean pressure p. Fig. 5 demonstrates exemplary for sand L11 that the curves of $G_{\max}$ versus p are linear in the double-logarithmic scale, that means they obey the proportionality $G_{\max} \sim p^n$.

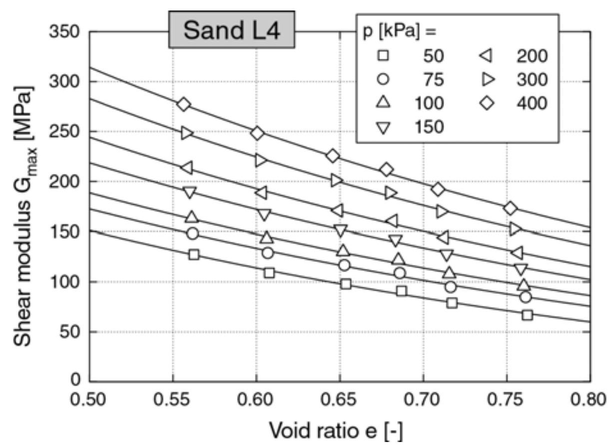

Fig. 4: Small-strain shear modulus G_{max} as a function of void ratio e and mean pressure p for sand L4

The RC tests on the materials L1 to L8 with C_u = 1.5 and with different mean grain sizes in the range $0.1 \leq d_{50} \leq 6$ mm revealed that for constant values of void ratio and mean pressure, $G_{\max}$ does not depend on d_{50} (Fig. 6). The slightly lower $G_{\max}$-values for the gravel L8 can be explained with an insufficient interlocking between the tested material and the end plates which were glued with coarse sand (Martinez, 2007). The observed d_{50}-independence of $G_{\max}$ is in good agreement with the test results of Iwasaki and Tatsuoka (1977).

The RC tests on the sands L24 to L26 (d_{50} = 0.2 mm and $2 \leq C_u \leq 3$), L10 to L16 (d_{50} = 0.6 mm and $2 \leq C_u \leq 8$) and L17 to L23 (d_{50} = 2 mm and $2 \leq C_u \leq 8$) showed that for e,p = constant, the small-strain shear modulus $G_{\max}$ significantly decreases with an increasing coefficient of uniformity C_u (Figs. 7 and 8). On average, the shear modulus at C_u = 8 amounts only 50 % of the value at C_u = 1.5. Fig. 7 also contains the curves predicted by Eq. (2). Obviously, Hardin's equation with its commonly used constants overestimates the G_{max}-values of well-graded sands while the shear modulus of uniform sands may be underestimated.

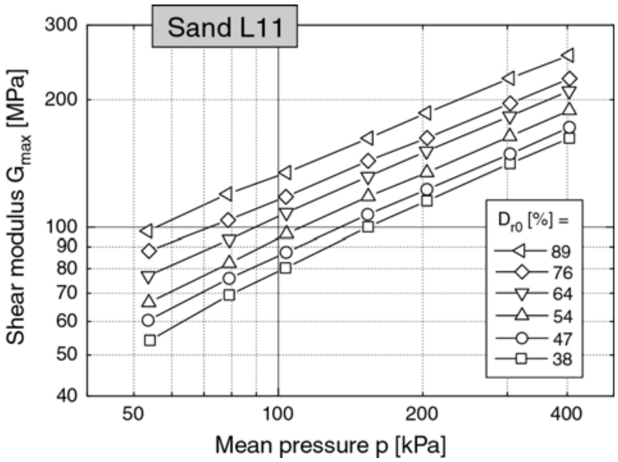

Fig. 5: Small-strain shear modulus G_{max} as a function of mean pressure p for sand L11

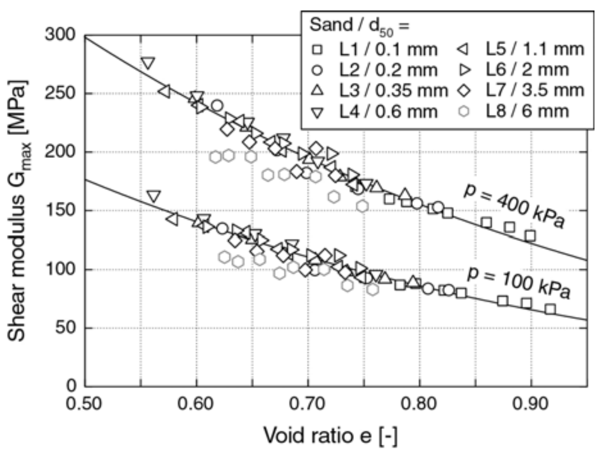

Fig. 6: No dependence of G_{max} on mean grain size d_{50}, Wichtmann and Triantafyllidis (2009a)

Eq. (2) has been fitted to the data of each sand in order to determine the parameters *A*, *a* and *n*. The correlations of these parameters with the coefficient of uniformity C_u (Fig. 9) can be described by the following equations:

$$a = 1.94 \exp(-0.066\, C_u) \tag{6}$$

$$n = 0.40\, (C_u)^{0.18} \tag{7}$$

$$A = 1563 + 3.13\, (C_u)^{2.98} \tag{8}$$

The diagrams in Fig. 10 confirm the good agreement between the measured shear moduli and the G_{max}-values predicted by Eq. (2) with the correlations (6) to (8). The diagram in Fig. 10d reveals that the proposed correlations (6) to (8) work well also for the sand-gravel mixtures L27 and L28, that means for linear grain size distribution curves with coefficients of uniformity up to approx. 16. Wichtmann and Triantafyllidis (2009a) demonstrated that Eq. (2) with the new correlations (6) to (8) also predicts well the shear moduli for various sands documented in the literature.

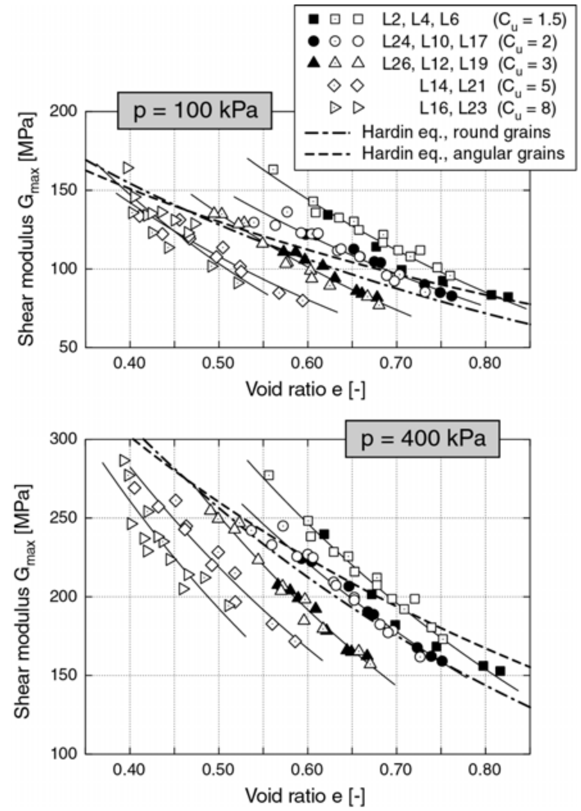

Fig. 7: Comparison of curves $G_{max}(e)$ measured for sands with different C_u-values, shown for p = 100 and 400 kPa, Wichtmann and Triantafyllidis (2009a)

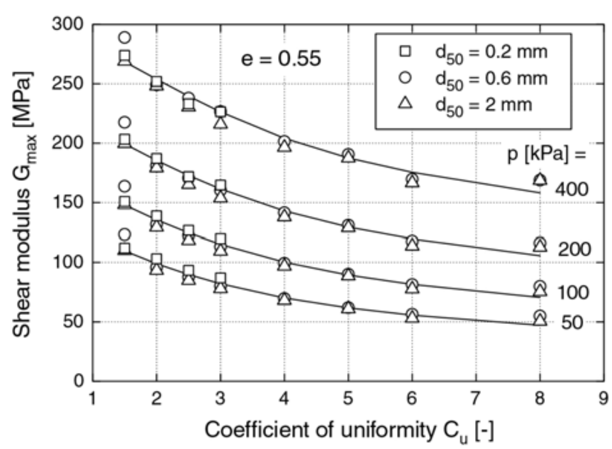

Fig. 8: Decrease of G_{max} with increasing coefficient of uniformity C_u, data for a constant void ratio e = 0.55, Wichtmann and Triantafyllidis (2009a)

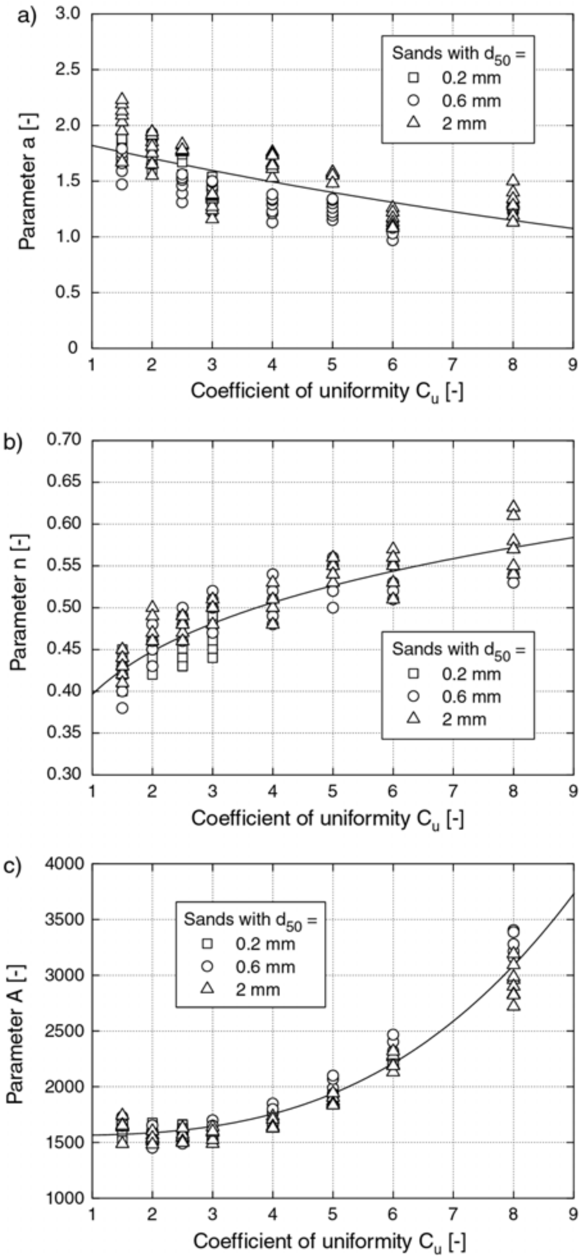

Fig. 9: Correlations of the parameters A, a and n of Eq. (2) with the coefficient of uniformity C_u, Wichtmann and Triantafyllidis (2009a)

The void-ratio-dependence of the modulus coefficient $K_{2,\max}$ in Eq. (3) can be described by

$$K_{2,max} = A_k \frac{(a_k - e)^2}{1+e} \tag{9}$$

The following correlations of the parameters A_k and a_k in Eq. (9) with C_u could be formulated based on the test data:

$$a_k = 1.94 \exp(-0.066\ C_u) \tag{10}$$
$$A_k = 69.9 + 0.21\ (C_u)^{2.84} \tag{11}$$

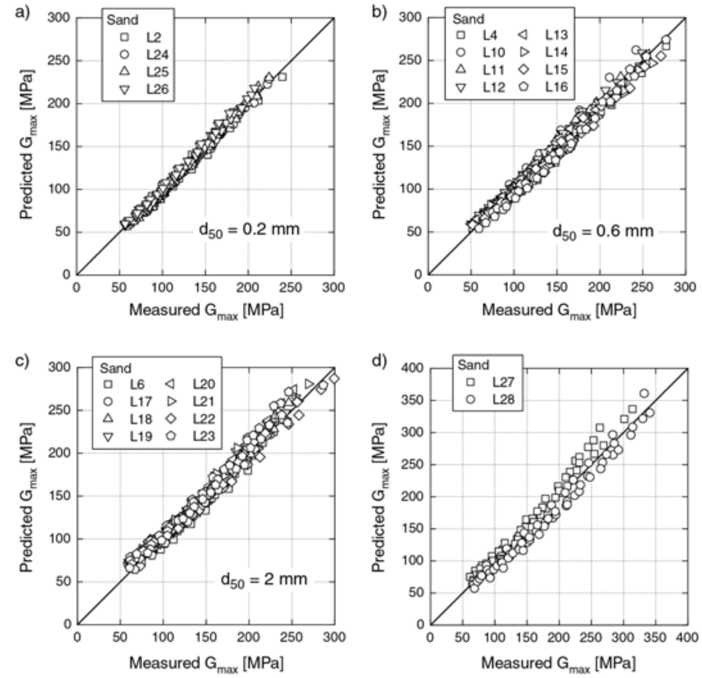

Fig. 10: Comparison of measured shear moduli G_{max} with the values predicted by Eq. (2) using the new correlations (6) to (8)

Due to the fixed exponent of the pressure-dependence, the $G_{\max}$-values predicted by Eqs. (3) and (9) to (11) are slightly less accurate than those obtained from Eq. (2) with the correlations (6) to (8).

For a constant relative density D_r the influence of the coefficient of uniformity on $G_{\max}$ is significantly smaller than for a constant void ratio. This is due to the fact that the minimum and maximum void ratios $e_{\min}$ and $e_{\max}$ decrease with increasing C_u. The following correlation between $G_{\max}$ and D_r has been derived (Wichtmann and Triantafyllidis, 2009a):

$$G_{\max} = A_D \frac{1 + D_r/100}{(a_D - D_r/100)^2} (p_{atm})^{1-n_D}\ p^{n_D} \tag{12}$$

with constants A_D = 177000, a_D = 17.3 and n_D = 0.48. The prediction of Eq. (12) is less accurate than that of Eq. (2) with (6) to (8). However, Eq. (12) may suffice for practical purposes.

Wichtmann and Triantafyllidis (2009a) provide a micromechanical explanation of the d_{50}-independence of $G_{\max}$ and of the decrease of $G_{\max}$ with increasing C_u. They also discuss corrections to the laboratory data in order to apply the new correlations to in-situ conditions, considering the degree of saturation, aging effects, etc.

Influence of fines content on $G_{\max}$

The RC tests on sands F1 to F6 show a strong decrease of $G_{\max}$ with increasing fines content in the range $FC \leq 10$ %. This becomes obvious from Fig. 11, where the curves $G_{\max}(e)$ of the sands with different fines contents are compared for p = 400 kPa. In Fig. 12 the G_{max}-values for a constant void ratio e = 0.825 are plotted versus FC. On average, the G_{max}-values of a sand with a fines content of 10 % amount only 57 % of the values for clean sand, measured for the same void ratio and the same pressure.

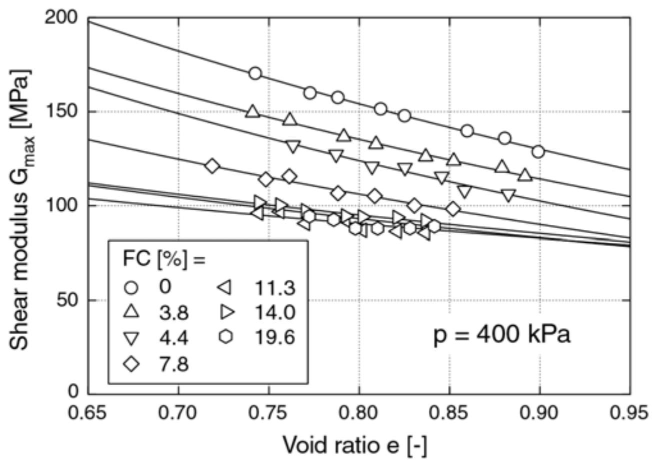

Fig. 11: Comparison of curves $G_{max}(e)$ for the sands with different fines contents

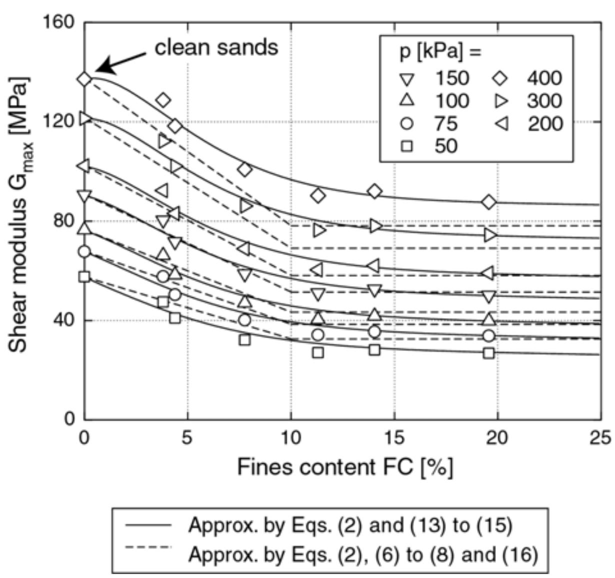

Fig. 12: Decrease of small-strain shear modulus G_{max} with incrasing fines content, data for a constant void ratio e = 0.825

The parameters A, a and n of Eq. (2) were correlated with the fines content (see the exemplary plot of a versus FC in Fig. 13). The following extension of Eqs. (6) to (8) by the influence of the fines content is proposed:

$$a = 1.94 \exp(-0.066\, C_u) \exp(0.065\, FC) \tag{13}$$

$$n = 0.40\, (C_u)^{0.18}\, [1 + 0.116 \ln(1 + \mathrm{FC})] \tag{14}$$

$$A = 0.5\, [1563 + 3.13\, (C_u)^{2.98}]\, [\exp(-0.30\, \mathrm{FC}^{1.10}) + \exp(-0.28\, \mathrm{FC}^{0.85})] \tag{15}$$

A very flexible function for the parameter A is necessary. For fines contents FC > 10 %, an average inclination C_u^{av} (see the scheme in Fig. 2d) of the grain size distribution curve in the range of grain sizes d > 0.063 mm has to be chosen for the coefficient of uniformity C_u in Eqs. (13) to (15). The good approximation of the test data by Eq. (2) with the correlations (13) to (15) can be seen in Fig. 12, where the prediction is given as the solid curves.

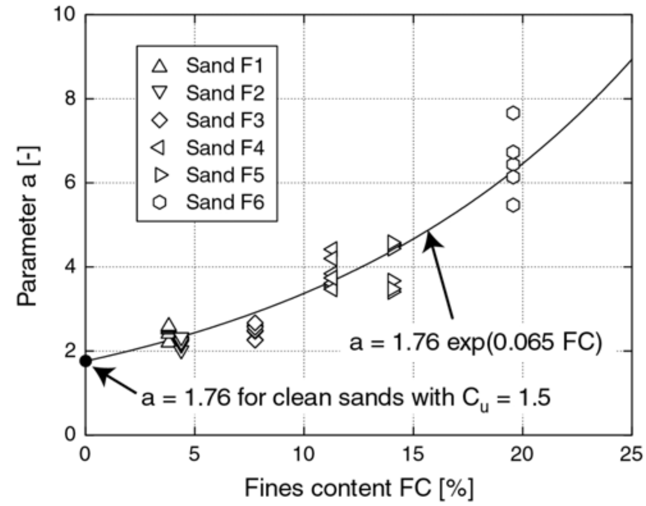

Fig. 13: Parameter a of Eq. (2) as a function of fines content

Alternatively, the small-strain shear modulus obtained from Eq. (2) with the correlations (6) to (8) can be reduced by a factor f_r which depends on the fines content:

$$f_r(FC) = \begin{cases} 1 - 0.043 FC & \text{for} \quad FC \leq 10\,\% \\ 0.57 & \text{for} \quad FC > 10\,\% \end{cases} \tag{16}$$

The void ratio- and pressure-dependence of f_r is neglected in Eq. (16). The prediction of G_{max} using Eq. (2) with (6) to (8) and with the reduction factor f_r from Eq. (16) is shown in Fig. 12 as the dashed curves. The quality of prediction is worse than that of Eq. (2) with the correlations (13) to (15).

For the sands with different fines content, G_{max} does not correlate with relative density D_r (Fig. 14).

Influence of d_{50} and C_u on M_{max}

The well-known increase of the small-strain constrained elastic modulus $M_{max} = \rho(v_P)^2$ with decreasing void ratio and with increasing pressure is shown exemplary for sand L2 in Fig. 15.

The P-wave measurements on the sands L1 to L7 showed that for e,p = constant, the small-strain constrained elastic modulus M_{max} does not depend on mean grain size (Fig. 16). Fig. 17 demonstrates based on the data measured for sands L10 to L26, that M_{max} decreases with increasing coefficient of uniformity.

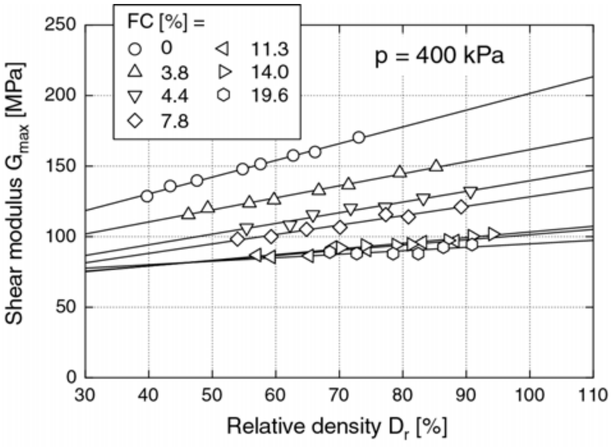

Fig. 14: G_{max} of the sands with different fines contents as a function of relative density D_r.

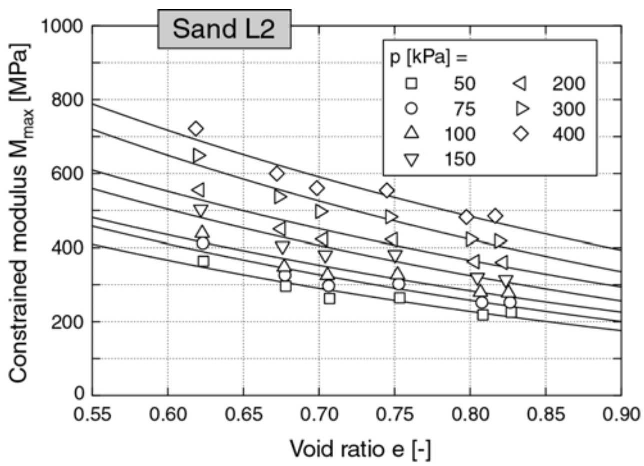

Fig. 15: Small-strain constrained elastic modulus M_{max} as a function of void ratio e and mean pressure p

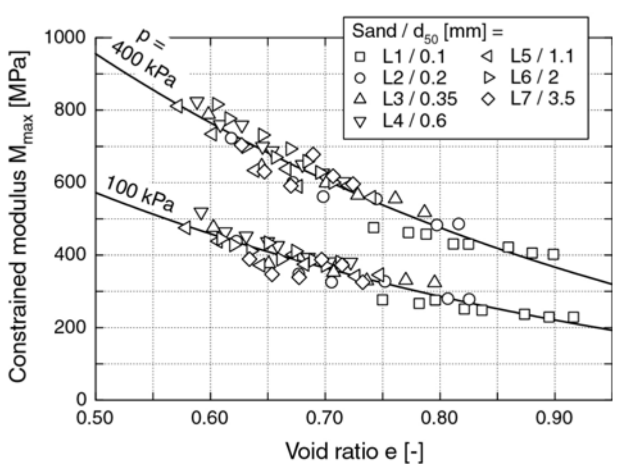

Fig. 16: No influence of mean grain size d_{50} on constrained elastic modulus M_{max}, Wichtmann and Triantafyllidis (2009b)

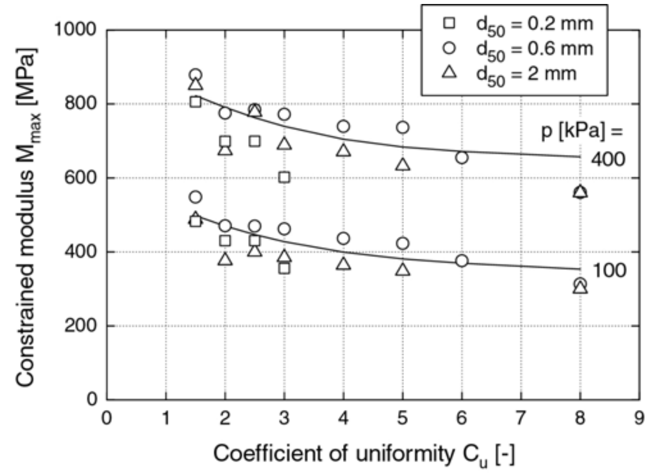

Fig. 17: Decrease of constrained elastic modulus M_{max} with increasing coefficient of uniformity, Wichtmann and Triantafyllidis (2009b)

Eq. (2) with $M_{\max}$ instead of $G_{\max}$ has been fitted to the experimental data for each sand:

$$M_{\max} = A \, \frac{(a-e)^2}{1+e} \, (p_{atm})^{1-n} \; p^n \tag{17}$$

The parameters A, a and n of Eq. (17) could be correlated with C_u using Eqs. (6) to (8) with different constants:

$$a = 2.16 \exp(-0.055\ C_u) \tag{18}$$
$$n = 0.344\ (C_u)^{0.126} \tag{19}$$
$$A = 3655 + 26.7\ (C_u)^{2.42} \tag{20}$$

The relative good approximation of the test data by Eq. (17) with the correlations (18) to (20) is demonstrated in Fig. 18 where the predicted $M_{\max}$-values are plotted versus the measured ones. The scatter of data is slightly larger than in the case of $G_{\max}$ (Fig. 10).

Alternatively, $M_{\max}$ can be estimated based on relative density D_r:

$$M_{\max} = A_D \; (1 + a_D \; D_r / 100) \, (p_{atm})^{1-n_D} \; p^{n_D} \tag{21}$$

with constants A_D = 2516, a_D = 0.92 and n_D = 0.39. The $M_{\max}$-values predicted by Eq. (21) are less accurate than those obtained from Eq. (17) with (18) to (20). However, Eq. (21) may suffice for practical purposes.

Fig. 19 presents Poisson's ratio ν for a constant void ratio e = 0.55 as a function of the coefficient of uniformity. Poisson's ratio was calculated using Eq. (2) with the correlations (6) to (8) and Eq. (17) with the correlations (18) to (20). Obviously, ν increases with increasing coefficient of uniformity and decreases slightly with increasing pressure.

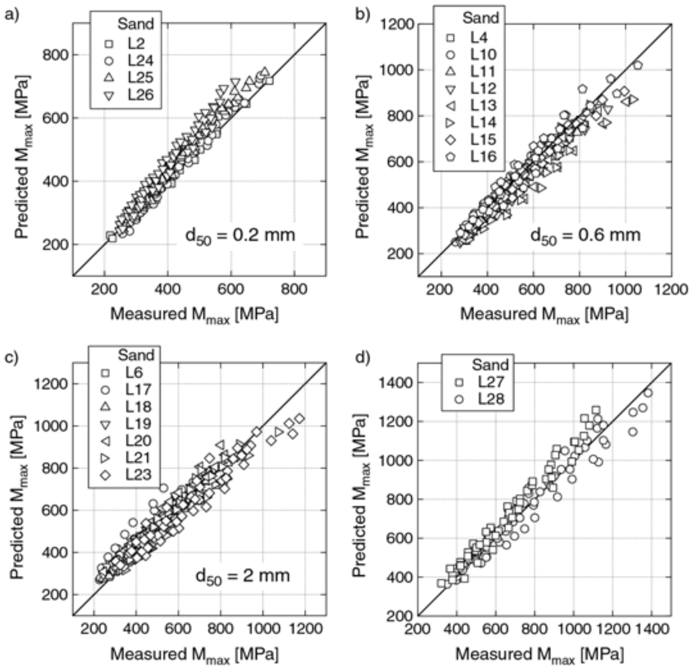

Fig. 18: Comparison of measured constrained elastic moduli M_{max} with the values predicted by Eq. (17) with the new correlations (18) to (20)

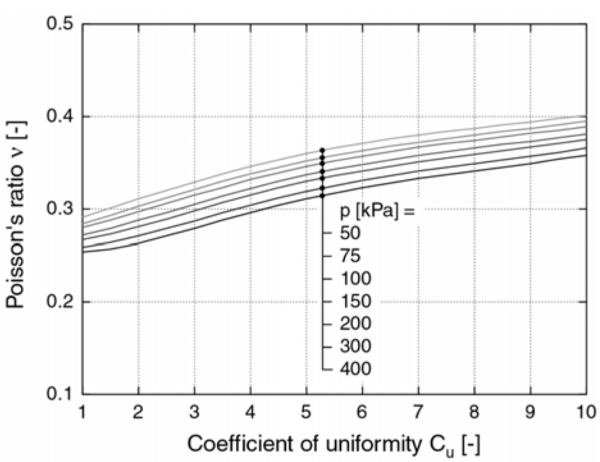

Fig. 19: Poisson's ratio ν for a constant void ratio e = 0.55 as a function of the coefficient of uniformity, Wichtmann and Triantafyllidis (2009b)

Influence of fines content on $M_{\max}$

Similar to $G_{\max}$, also $M_{\max}$ decreases with increasing fines content in the range $FC \leq 10$ % (Fig. 20). On average, the $M_{\max}$-values for $FC = 10$ % amount 60 % of the values for clean sand.

The following extension of the correlations (18) to (20) has been developed considering the influence of the fines content:

$$a = 2.16 \exp(-0.055\, C_u)\ (1 + 0.116\, FC) \tag{22}$$

$$n = 0.344\, (C_u)^{0.126}\, [1 + 0.125 \ln(1 + \mathrm{FC})] \tag{23}$$

$$A = 0.5\, [3655 + 26.7\, (C_u)^{2.42}]\, [\exp(-0.42\, \mathrm{FC}^{1.10}) + \exp(-0.52\, \mathrm{FC}^{0.60})] \tag{24}$$

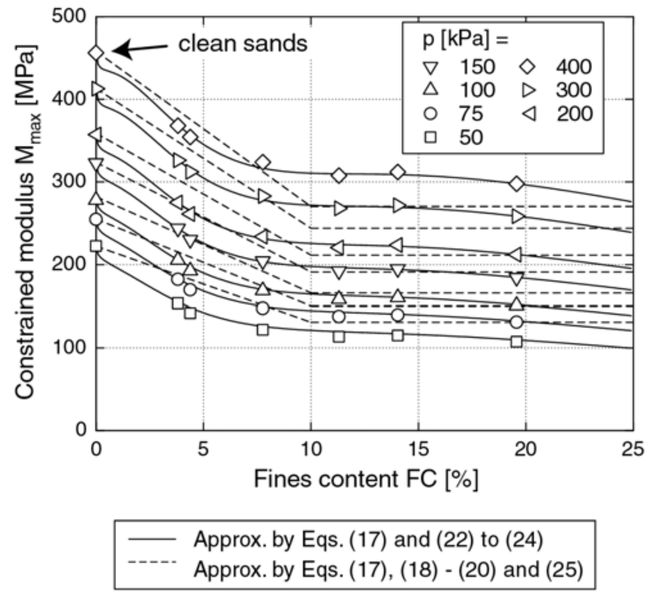

Fig 20: Decrease of small-strain constrained elastic modulus M_{max} with increasing fines content, data for a constant void ratio e = 0.825

The good prediction of the measured $M_{\max}$-values by Eq. (17) with the correlations (22) to (24) is demonstrated in Fig. 20, where the prediction is shown as solid curves.

For a simplified procedure, the constrained elastic modulus $M_{\max}$ obtained for clean sands from Eq. (17) with (18) to (20) can be reduced by a factor f_r:

$$f_r(FC) = \begin{cases} 1 - 0.041 FC & \text{for} \quad FC \leq 10\,\% \\ 0.59 & \text{for} \quad FC > 10\,\% \end{cases} \tag{25}$$

The prediction of $M_{\max}$ using Eq. (17) with (18) to (20) and with the reduction factor f_r from Eq. (25) is shown in Fig. 20 as the dashed curves.

For the sands with a fines content Poisson's ratio ν has been calculated from Eq. (2) with (13) to (15) and from Eq. (17) with (22) to (24). The small dependence of ν on the fines content (Fig. 21) can be neglected for practical purposes.

Influence of d_{50} and C_u on the curves $G(\gamma)/G_{\max}$ and $D(\gamma)$

Typical curves of shear modulus G versus shear strain amplitude γ for four different pressures are shown in Fig. 22a, exemplary for sand L11. In Fig. 22b the curves have been normalized by their maximum value $G_{\max}$ at small strain amplitudes. The well-known larger modulus degradation for smaller pressures is obvious in Fig. 22b. The curves lay within the range specified as typical by Seed et al. (1986). Fig. 23 presents normalized curves $G(\gamma)/G_{\max}$ measured at p = 400 kPa for different relative densities. Obviously, the curves $G(\gamma)/G_{\max}$ do not depend on density.

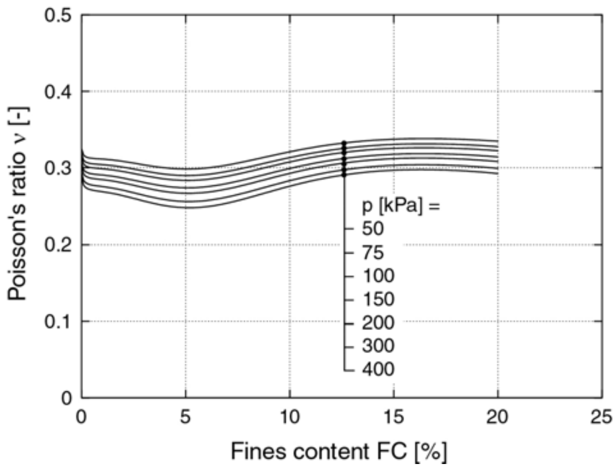

Fig. 21: Poisson's ratio ν as a function of fines content

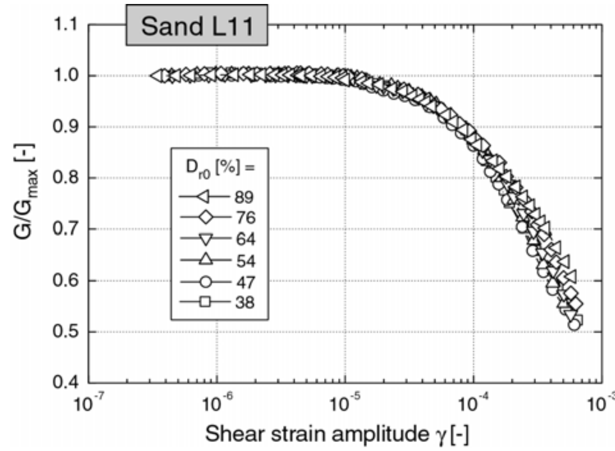

Fig. 23: Typical curves $G(\gamma)/G_{max}$ at p = 400 kPa for different relative densities, shown exemplary for sand L11

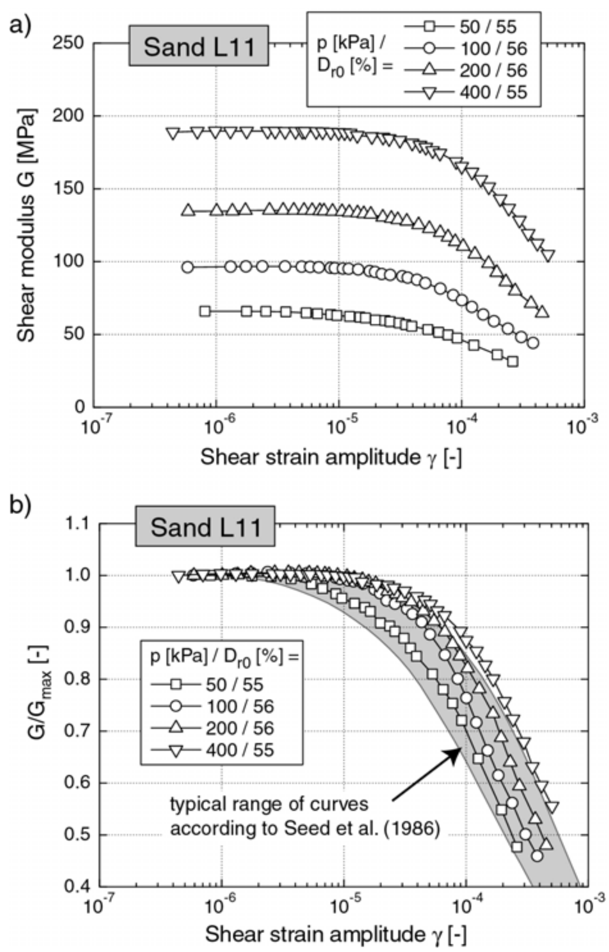

Fig. 22: Typical curves $G(\gamma)$ and $G(\gamma)/G_{max}$ for four different pressures, shown exemplary for sand L11

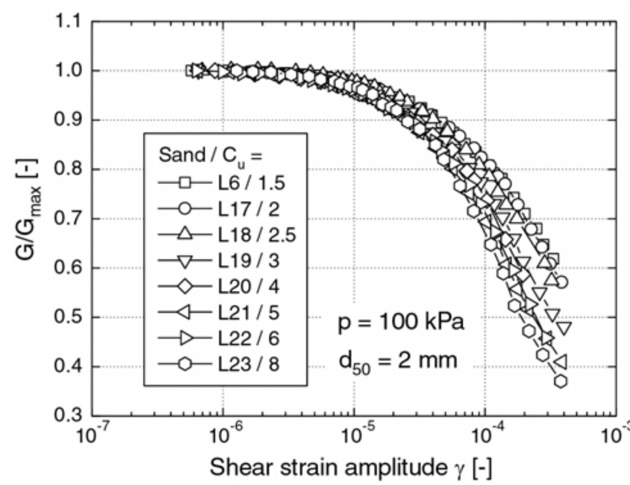

Fig 24: Comparison of curves $G(\gamma)/G_{max}$ measured for eight sands with different coefficients of uniformity C_u

Fig. 24 shows a comparison of the curves $G(\gamma)/G_{\max}$ measured for eight sands with different C_u-values. Obviously, the modulus degradation with increasing shear strain amplitude becomes larger with increasing coefficient of uniformity. This is also evident from Fig. 25 where the normalized shear modulus $G/G_{\max}$ is plotted versus C_u. For a certain shear strain amplitude $G/G_{\max}$ decreases with increasing coefficient of uniformity. The influence of the mean grain size on the curves $G(\gamma)/G_{\max}$ is rather small.

In order to obtain the reference shear strain γ_r (Eq. (5)), the peak friction angle φ_P was determined in triaxial tests with monotonic compression. For each material the density-dependence of φ_P was examined in at least three tests with different initial relative densities. From the peak friction angle the maximum shear stress $\tau_{\max}$ was calculated. Fig. 26 shows typical curves of the modulus reduction factor $G/G_{\max}$ as a function of the normalized shear strain amplitude γ/γ_r. For each tested material, Eq. (4) was fitted to such data. Setting b = 1 in Eq. (4) is sufficient in order to describe the shear modulus degradation curves (see also Hardin and Kalinski, 2005). The parameter a in Eq. (4) could be correlated with the coefficient of uniformity C_u (Fig. 27):

$$a = 1.070 \ln(C_u) \qquad (26)$$

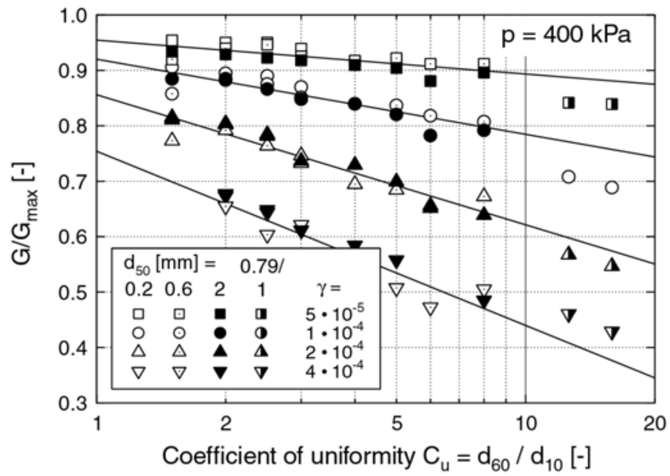

Fig 25: Factor G/G_{max} for different shear strain amplitudes as a function of C_u

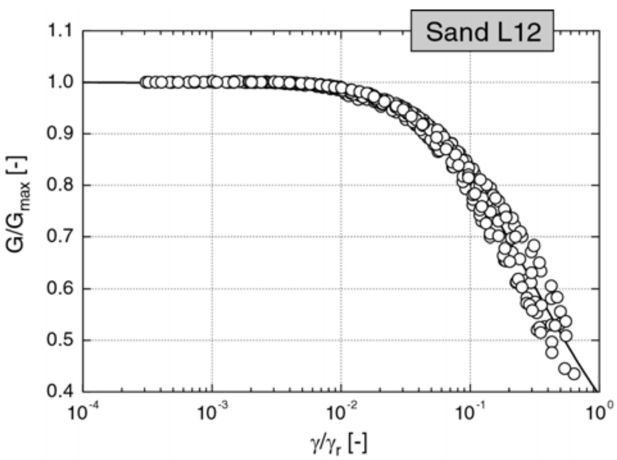

Fig 26: Curves $G(\gamma/\gamma_r)/G_{max}$, shown exemplary for sand L12

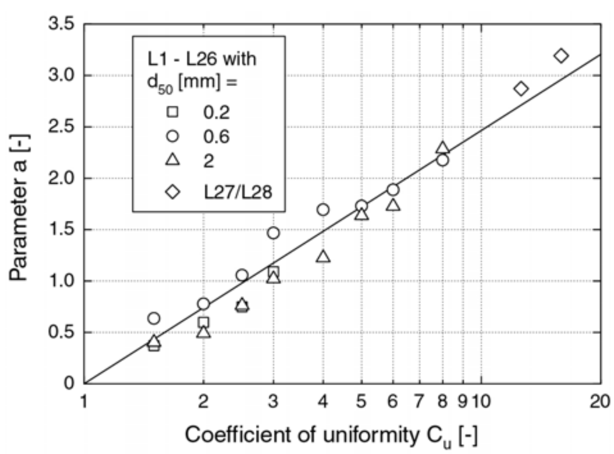

Fig 27: Correlation of the parameter a in Eq. (4) with the coefficient of uniformity

Typical curves of damping ratio D versus shear strain amplitude γ are given in Fig. 28. The damping ratio increases with decreasing pressure, but does not depend on density. A comparison of the damping ratios measured for the sands L1 to L8 revealed that D does not significantly depend on mean grain size.

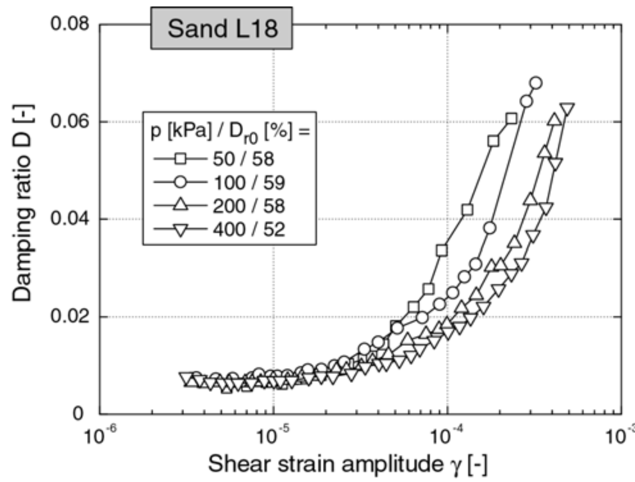

Fig 28: Damping ratio D as a function of shear strain amplitude, shown exemplary for sand L18

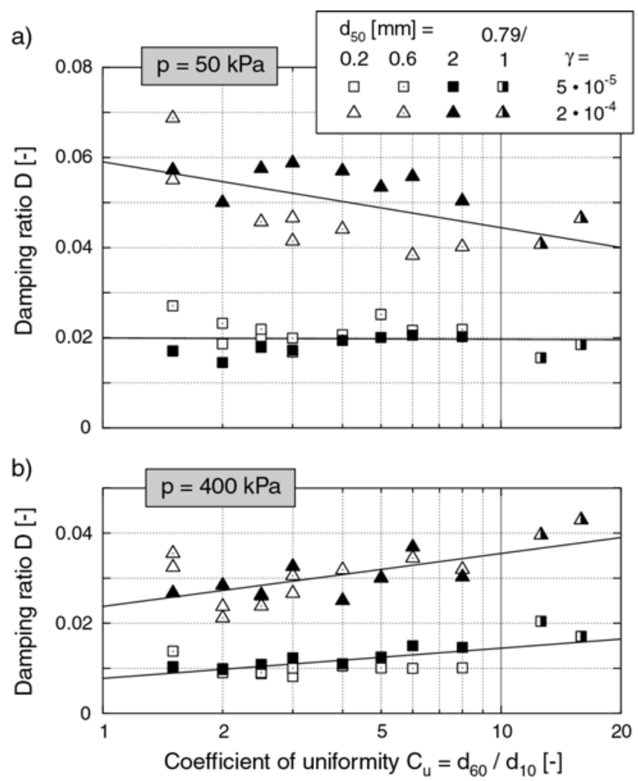

Fig 29: Damping ratio D for two different shear strain amplitudes and two different pressures as a function of the coefficient of uniformity

The influence of the coefficient of uniformity on damping ratio depends on the shear strain amplitude and on pressure. For larger pressures (Fig 29b), D increases with C_u, independently of the shear strain amplitude. For smaller pressures (Fig. 29a) D is almost independent of C_u for small shear strain amplitudes while a decrease of D with C_u was observed at larger γ-values.

From the curves of the settlement of the specimen versus shear strain amplitude (see a typical test result in Fig. 30) the threshold shear strain amplitude γ_{tv} at the onset of settlement was determined. The threshold shear strain amplitude γ_{tl} at the transition from the linear to the nonlinear elastic behavior was defined as the amplitude for which the shear modulus has decreased to 99 % of its initial value (i.e. $G = 0.99\ G_{\max}$). A clear dependence of the threshold amplitudes γ_{tl} and γ_{tv} on the mean grain size and on the coefficient of uniformity could not be found (Fig. 31).

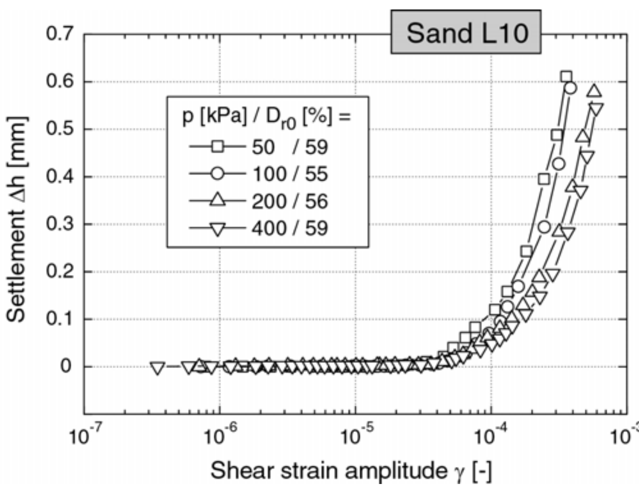

Fig 30: Settlement of the specimen as a function of shear strain amplitude, shown exemplary for sand L10

Influence of fines content on the curves $G(\gamma)/G_{\max}$ and $D(\gamma)$

Hardly no influence of the fines content on the curves $G(\gamma)/G_{\max}$ and $D(\gamma)$ could be found in the RC tests on sands F1 to F6. For a certain shear strain amplitude γ, the factor $G/G_{\max}$ does not depend on FC (Fig. 32). However, due to the decrease of $G_{\max}$ with increasing FC, the reference shear strain γ_r significantly increases with fines content, resulting in an increase of the parameter a in Eq. (4). The following extension of Eq. (26) is proposed based on the data in Fig. 33:

$$a = 1.070 \ln(C_u) \exp(0.053\ FC) \tag{27}$$

For small pressures (p = 50 kPa) the damping ratio D decreases by almost a factor 4 from FC = 0 % to FC = 10 %. For larger fines contents the damping ratio stays almost constant. For larger pressures (p = 400 kPa) the decrease of D with FC is less pronounced.

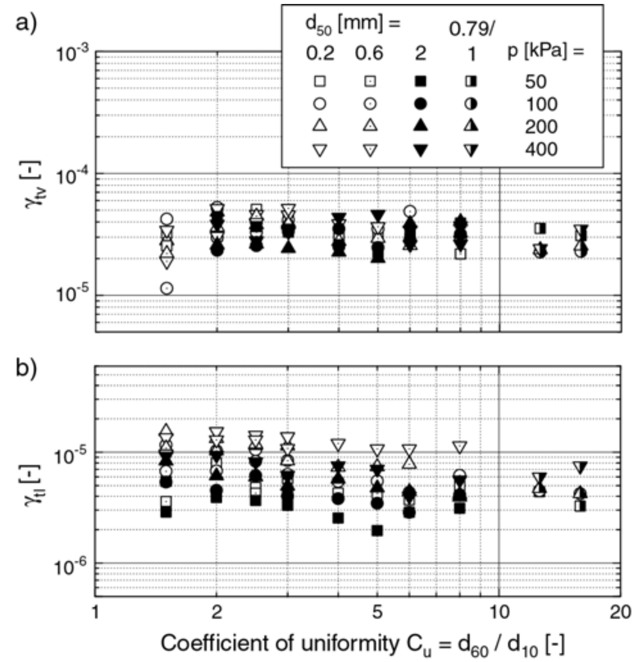

Fig 31: Threshold shear strain amplitudes γ_{tl} (onset of shear modulus degradation, defined at G = 0.99 G_{max}) and γ_{tv} (onset of settlement)

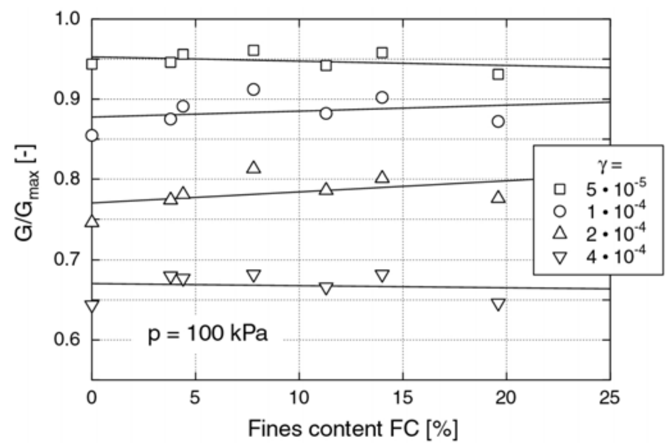

Fig 32: Factor G/G_{max} for different shear strain amplitudes as a function of fines content

The linear elastic threshold shear strain amplitude γ_{tl} is hardly influenced by the fines content. However, there is an influence of FC on the cumulative threshold shear strain amplitude γ_{tv}. With increasing fines content the accumulation of residual strain starts at larger shear strain amplitudes, that means γ_{tv} increases with increasing FC. For $FC \geq 10$ %, γ_{tv} is approximately 10^{-4} (compare the lower γ_{tv}-values for clean sands in Fig. 31a). γ_{tv} remains constant if the fines content is further increased.

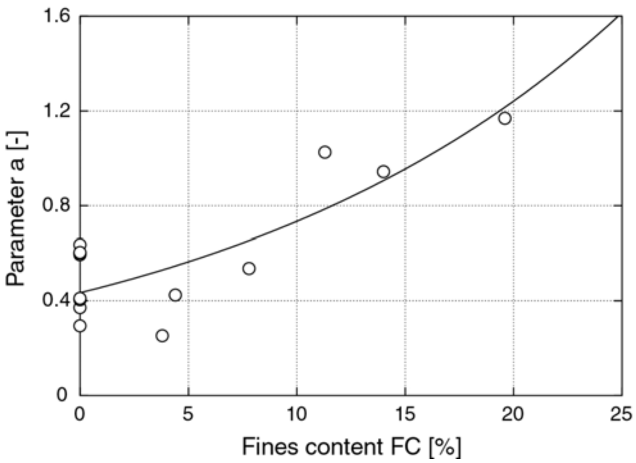

Fig 33: Increase of parameter a in Eq. (4) with increasing fines content

SUMMARY, CONCLUSIONS AND OUTLOOK

Approx. 350 resonant column tests with additional P-wave measurements have been performed on 33 quartz sands with different grain size distribution curves. The small-strain shear modulus $G_{\max}$ and the small-strain constrained elastic modulus $M_{\max}$ were found to decrease significantly with increasing coefficient of uniformity $C_u = d_{60}/d_{10}$ of the grain size distribution curve. A further decrease results from an increasing fines content FC. In contrast, $G_{\max}$ and $M_{\max}$ are not affected by the mean grain size d_{50}. An empirical equation originally proposed by Hardin has been extended by the influence of the grain size distribution curve. For that purpose the parameters of Hardin's equation have been correlated with C_u and FC. Correlations of $G_{\max}$ and $M_{\max}$ with relative density were also developed but are slightly less accurate. Poisson's ratio ν was found to increase with increasing coefficient of uniformity. For practical purposes it can be assumed independent of the fines content.

For a certain shear strain amplitude, the modulus degradation factor $G(\gamma)/G_{\max}$ was found smaller for larger coefficients of uniformity. However, the factor does not depend on the fines content. An empirical formula for the modulus degradation factor has been extended by the influence of the grain size distribution curve. Damping ratio D decreases or increases with increasing C_u, depending on pressure and on the shear strain amplitude. A fines content significantly reduces the damping ratio, at least for lower pressures. The linear elastic threshold shear strain amplitude γ_{tl} depends neither on C_u nor on FC. The cumulative threshold shear strain amplitude γ_{tv} is not affected by the coefficient of uniformity, but increases with increasing fines content.

At present bilinear, step-shaped, S-shaped or other naturally shaped grain size distribution curves of practical relevance are being tested. The applicability of the novel correlations for $G_{\max}$, $M_{\max}$ and the modulus degradation factor to arbitrary grain size distribution curves will be examined.

ACKNOWLEDGEMENT

The presented study has been performed within the framework of the project "Influence of the coefficient of uniformity of the grain size distribution curve and of the fines content on the dynamic properties of non-cohesive soils" funded by the German Research Council (DFG, project No. TR218/11-1). The authors are grateful to DFG for the financial support. The RC tests have been performed during the former work of the authors at Ruhr-University Bochum, Germany. The authors gratefully acknowledge the help of the diploma thesis students R. Martinez, F. Durán-Graeff, E. Giolo and M. Navarrete Hernández.

REFERENCES

Hardin, B.O. and Richart Jr., F.E. [1963]. "Elastic wave velocities in granular soils", Journal of the Soil Mechanics and Foundations Division, ASCE, Vol. 89, No. SM1, pp.33-65.

Hardin, B.O. and Black, W.L. [1966]. "Sand stiffness under various triaxial stresses", Journal of the Soil Mechanics and Foundations Division, ASCE, Vol. 92, No. SM2, pp. 27-42.

Hardin, B.O. and Kalinski, M.E. [2005]. "Estimating the shear modulus of gravelly soils", Journal of Geotechnical and Geoenvironmental Engineering, ASCE, Vol. 131, No. 7, pp. 867-875.

Iwasaki, T. and Tatsuoka, F. [1977]. "Effects of grain size and grading on dynamic shear moduli of sands", Soils and Foundations, Vol. 17, No. 3, pp. 19-35.

Martinez, R. [2007]: "Influence of the grain size distribution curve on the stiffness and the damping ratio of non-cohesive soils at small strains" (in German), Diploma thesis, Institute of Soil Mechanics and Foundation Engineering, Ruhr-University Bochum, Germany.

Seed, H.B. and Idriss, I.M. [1970]. "Soil moduli and damping factors for dynamic response analyses", Technical Report EERC 70-10, Earthquake Engineering Research Center, University of California, Berkeley.

Seed, H.B., Wong, R.T., Idriss, I.M. and Tokimatsu, K. [1986]. "Moduli and damping factors for dynamic analyses of cohesionless soil", Journal of Geotechnical Engineering, ASCE, Vol. 112, No. 11, pp. 1016-1032.

Wichtmann, T. and Triantafyllidis, T. [2009a], "Influence of the grain size distribution curve of quartz sand on the small strain shear modulus $G_{\max}$" (in print), Journal of Geotechnical and Geoenvironmental Engineering, ASCE, Vol. 135, No. 10.

Wichtmann, T. and Triantafyllidis, T. [2009b], "On the influence of the grain size distribution curve on P-wave velocity, constrained elastic modulus $M_{\max}$ and Poisson's ratio of quartz sands", submitted to Soil Dynamics and Earthquake Engineering.